High Energy Electron-Proton Physics at HERA

H1 COLLABORATION PROPOSAL 750

The Universities of Birmingham, Lancaster, Liverpool, and Manchester, Queen Mary and Westfield College, University of London, and Rutherford Appleton Laboratory

with

RWTH Aachen (I and III Inst.), Humboldt Univ. Berlin, Universities of Brussels, Cracow and Dortmund, JINR Dubna, CEA Saclay, DESY–Hamburg, DESY–Zeuthen, Universities of Hamburg (II Inst.) and Heidelberg, MPI Heidelberg, Universities of Kiel, Košice, and Lund, CPPM-Marseille, ITEP Moscow, LPI Moscow, MPI Munich, LAL Orsay, Ecole Polytechnique, Universities of Paris VI, Paris VII, Prague, and Rome, PSI-Villigen, University of Wuppertal, ETH Zürich and University of Zürich

1 Introduction and Overview

The electron-proton collider HERA has recently completed its sixth year of running. After a long shutdown to enable the accelerator group and the individual experiments to carry out maintenance and upgrade work, luminosity was provided for the HERA experiments from August 1998. The proton beam energy was increased from 820 to 920 GeV and, for the first time since 1993, electrons were collided instead of positrons. A total luminosity of 9 pb^{-1} was delivered this year to H1 and ZEUS. HERA will run almost continuously from the beginning of 1999 until May 2000 and is expected to deliver an integrated luminosity in excess of $35\,\text{pb}^{-1}$ in that time. There will then be a shutdown of about nine months length during which major changes will be made to the HERA collider. These include the insertion of spin rotators before and after the H1 interaction region, which will allow *ep* collisions with defined lepton helicity to be studied, and the insertion of additional focussing elements close to and within H1. These latter will result in an increase in the attainable luminosity by a factor of about five to $150\,\text{pb}^{-1}$ per year.

During 1998 data taking, all of the H1 detector components which were designed and built by the UK groups, or for which they have some responsibility, were operational. These include the superconducting solenoid (RAL), the forward track detector (RAL, Glasgow, Lancaster, Liverpool, Manchester), the H1 central data acquisition system (RAL), the H1 central trigger control (RAL), the forward muon detector (Manchester) and its trigger (RAL, Birmingham, QMW), the timing system for the backward calorimeters (RAL, Birmingham, QMW), the forward time-of-flight scintillators (Manchester, QMW) and the data acquisition system of the silicon trackers (RAL).

The UK groups are heavily involved with preparations for the forthcoming long HERA shutdown. A major upgrade to the forward track detector was proposed to, and approved by, the Particle Physics Experiments Selection Panel in March 1998.

Notable H1 results presented in 1998 include:

- Inclusive neutral current and charged current cross-section measurements for Q^2 values up to 30 000 GeV^2.
- Stringent new limits on scalar lepto-quark production.
- Determination of the gluon density in the proton from deep inelastic charm production.
- Measurement of the open beauty cross-section in photoproduction.
- Measurements of jet production at low Q^2 which throw light on the partonic structure of the virtual photon.

This document is organised as follows: sections 2 to 6 focus on analysis work carried out by the H1-UK groups; section 7 discusses the performance of the detectors for which the H1-UK groups are responsible and describes progress with the preparations for the upgrade of the forward track detector.

2 High Q^2 Structure Function Measurements

The excellent performance of the HERA collider in recent years has allowed a substantial improvement in the precision of high Q^2 cross-section measurements. Such measurements greatly add to the understanding of both the strong and electroweak sectors of the standard model (SM). Deviations of these measurements from SM expectations could indicate new physics, as witnessed by the excitement caused by the observation in 1997 of a slight excess of events at very high Q^2 [1]. This section describes the high Q^2 neutral current (NC) and charged current (CC) cross-section measurements made using the data taken in the 1994-97 e^+p run of HERA.

In the SM the NC cross-section is related to the three structure functions F_2, F_L and xF_3, and for $e^+p \to e^+X$ is given by:

$$\frac{\mathrm{d}^2\sigma_{NC}}{\mathrm{d}x\ \mathrm{d}Q^2} = \frac{2\pi\alpha^2}{xQ^4}\left[Y_+F_2(x,Q^2) - y^2F_L(x,Q^2) - Y_-xF_3(x,Q^2)\right]. \qquad (1)$$

Here, F_2 is the generalised structure function which contains the effects of both photon and Z^0 exchange and F_L is the longitudinal structure function. The structure function F_3 becomes significant only when Q^2 is sufficiently large to make the effects of Z^0 exchange noticeable. The helicity dependence of electroweak interactions is contained in the functions $Y_\pm = 1 \pm (1-y)^2$. For the sake of simplicity, the NC results are sometimes presented in the form of the "reduced" cross-section, $\tilde{\sigma}_{NC} = (\mathrm{d}^2\sigma_{NC}/\mathrm{d}x\mathrm{d}Q^2)/(Y_+\kappa)$, where $\kappa = 2\pi\alpha^2/xQ^4$. Over most of the available phase space $\tilde{\sigma}_{NC}$ is to a very good approximation equal to F_2. Only at high y ($\gtrsim 0.6$) where the term involving F_L becomes large, and high Q^2 ($Q^2 \gtrsim 5\,000$ GeV^2) where xF_3 cannot be neglected, do the deviations from this approximation exceed 5%.

The CC cross-section can be written in terms of the above three structure functions in a manner analogous to the NC case [2], but can also be written in a compact form directly related to the parton density functions of the proton. To leading order this is:

$$\frac{\mathrm{d}^2\sigma_{CC}}{\mathrm{d}x\mathrm{d}Q^2} = \frac{G_F^2}{2\pi}\left(\frac{M_W^2}{M_W^2+Q^2}\right)^2\left((\bar{u}+\bar{c}) + (1-y)^2(d+s)\right), \qquad (2)$$

where G_F is the Fermi coupling constant, M_W the mass of the W boson and $\bar{u}$, $\bar{c}$, d and s are the quark densities in the proton. As for the NC case, a reduced CC cross section is employed which highlights the dependence of the CC cross section on the quark densities:

$$\tilde{\sigma}_{CC} \equiv \frac{2\pi x}{G_F^2}\left(\frac{M_W^2+Q^2}{M_W^2}\right)^2 \frac{\mathrm{d}^2\sigma}{\mathrm{d}x\mathrm{d}Q^2} = x\left((\bar{u}+\bar{c})+(1-y)^2(d+s)\right). \tag{3}$$

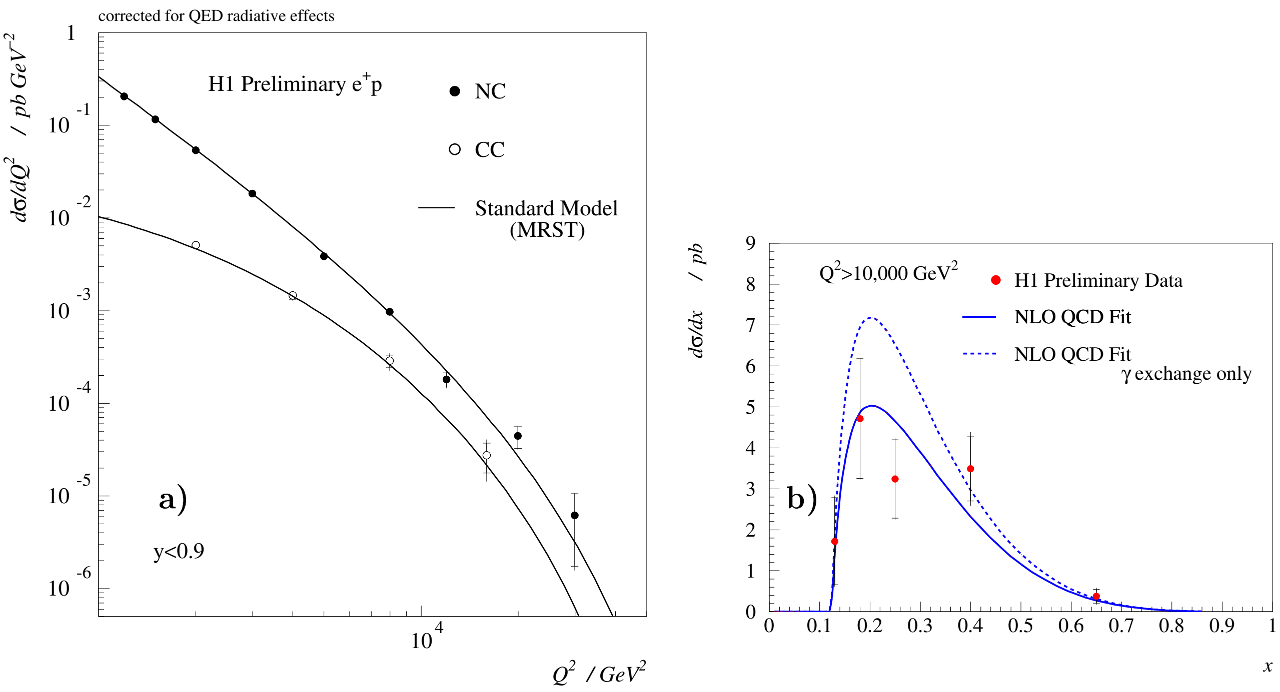

Figure 1: a) The single differential CC and NC cross sections together with the SM expectations. b) The NC cross section $\mathrm{d}\sigma/\mathrm{d}x$ for $Q^2 > 10\,000$ GeV^2, compared to the SM expectation (solid line) and to a model in which only photon exchange contributes (dashed line).

2.1 Single Differential Cross-Sections

The H1 measurements of the single differential CC and NC cross-sections, $\mathrm{d}\sigma/\mathrm{d}Q^2$, are shown in figure 1a). The rapid fall in the NC cross-section, by over six orders of magnitude over the measured range in Q^2, is well reproduced by the SM expectation [3, 4] with the exception of a slight excess over the SM at the very highest Q^2 values. The significance of this excess is reduced with the addition of the 1997 data compared to that observed in the 1994-1996 data alone.

The CC cross-section is seen to fall much less steeply at lower Q^2 values than the NC cross-section, due to the W mass in the propagator term (see equation 2). At $Q^2 \gtrsim M_W^2$, the two cross-sections become comparable in shape and magnitude, as expected in the SM. The remaining differences are related to the proportions of the quark flavours involved in NC and CC interactions and the densities of those flavours in the proton.

The CC cross-section measurements may be used to extract a value of M_W. Since CC interactions arise from the t channel exchange of a virtual W boson, the extracted value of M_W may be interpreted as a direct measurement in the space-like regime [5]. The value obtained ($M_W = 81.2 \pm 3.3(\mathrm{stat.}) \pm 4.3(\mathrm{sys.}) \pm 2.8(\mathrm{pdf})\mathrm{GeV}$) is in good agreement with the world average [6].

The influence of the exchange of heavy vector bosons is also observable for the first time in NC ep scattering in the new H1 data. In figure 1b) the cross section $\mathrm{d}\sigma/\mathrm{d}x$ is shown for

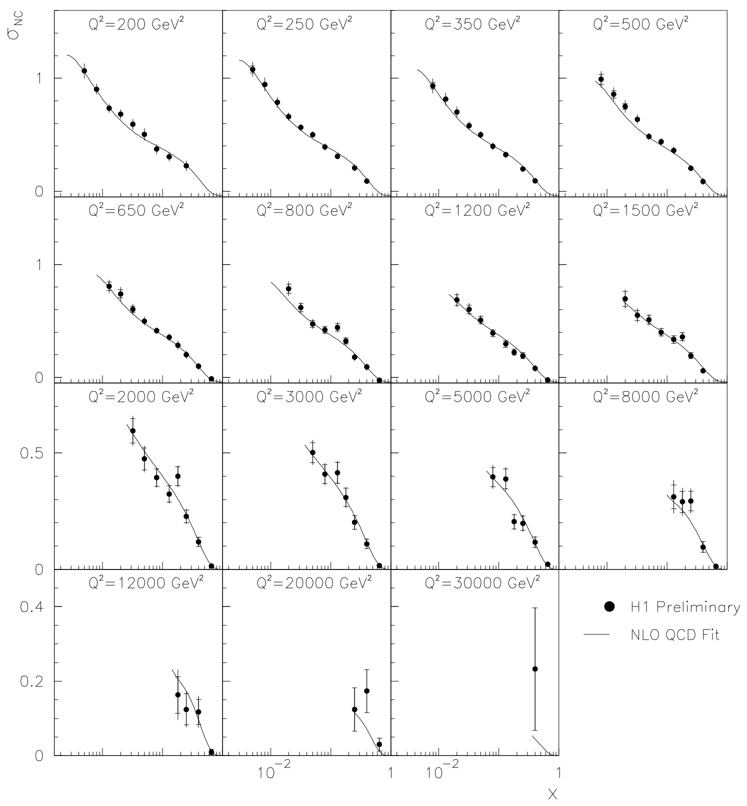

Figure 2: The NC double differential reduced cross section, compared to the standard model expectation.

$Q^2 > 10\,000$ GeV^2 together with the SM expectation and also a model in which there is no Z^0 exchange or γ/Z^0 interference. The suppression of the cross section caused by the negative γ/Z^0 interference is clearly visible.

2.2 Double Differential Cross-sections

The double differential CC and NC cross-sections $\mathrm{d}^2\sigma/\mathrm{d}x\mathrm{d}Q^2$ provide the full information available from the inclusive measurements. Figure 2 shows the double differential NC reduced cross-section measurement together with a QCD fit to this and lower Q^2 data. The new data extend both to higher Q^2 and to higher x than has been previously measured [7]. The data are in good agreement with the QCD fit, namely a steep rise towards low x, indicating an increasing parton density towards low momentum.

First measurements of the double differential CC cross-section have now been made by H1. In figure 3 the cross section is shown as a function of y for fixed x. The factor $(1-y)^2$ (see equation 2) effectively suppresses the contribution of the d quark at high y so that the high y CC cross section is sensitive only to the $\bar{u}$, and $\bar{c}$ densities. At high values of x, the sea quark density is small and so the cross section is largely dependent only on the d density. The charged current cross section, measured over a wide range of x and y is thus a powerful tool in the determination of the flavour composition of the proton. As can be seen in figure 3, the data are in good agreement with the QCD prediction over the whole kinematic range studied.

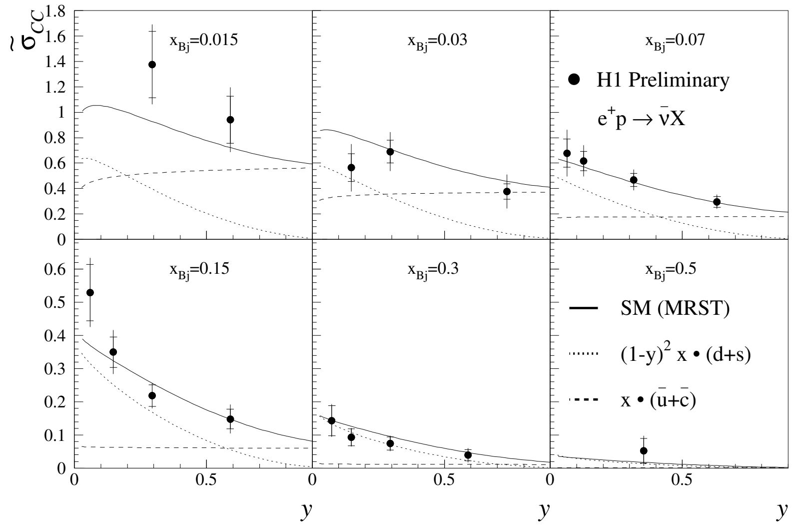

Figure 3: The CC double differential reduced cross section, shown as a function of x and y. The data are compared to the SM expectation with a decomposition into the various quark species that make up the CC cross section

3 Diffractive Hard Scattering

When discussing the success of the SM, it is often overlooked that the bulk of hadronic cross sections remain rather poorly understood within the gauge theory of the strong interaction, QCD. Before the advent of QCD, many aspects of hadronic interactions were understood in the framework of Regge phenomenology, which is based on the most general properties of the scattering matrix. In Regge models, diffractive (elastic, dissociative and, via the optical theorem, total) cross sections are described [8] at high energy in terms of the exchange of the leading vacuum singularity or *pomeron*. The relationship between Regge asymptotics and QCD is far from clear.

The lepton beam at HERA can be considered as a prolific source of high energy real and virtual photons, allowing diffractive scattering in the $\gamma^{(*)}p$ system to be studied. There are a variety of hard scales which are relevant to the problem, so HERA provides an excellent opportunity to study diffraction in regions in which perturbative QCD may be applicable. This leads to the exciting possibility of gaining an understanding of diffraction and the pomeron at the level of parton dynamics and of studying the transition between strong interactions which are perturbatively calculable and those which are not. UK physicists continue to be at the forefront of H1 investigations of diffractive phenomena.

3.1 The Diffractive Cross Section in DIS

Using data taken in 1994, H1 measured the cross section for the process $\gamma^* p \to XY$, where the systems X and Y are well separated in rapidity, for photon virtualities in the range $4.5 < Q^2 < 75$ GeV^2 [9]. The system Y has mass $M_Y < 1.6$ GeV and is usually a proton. The squared four-momentum transferred at the proton vertex is restricted to $|t| < 1$ GeV^2. The results were presented in terms of a diffractive structure function $F_2^{D(3)}(Q^2, \beta, x_{\mathbb{P}})$, where $x_{\mathbb{P}}$ can be interpreted as the fraction of the proton's momentum that is transferred to the pomeron and β as the fraction of the pomeron's momentum that is carried by the quark coupling to the photon. The inclusive diffractive DIS process was shown to be dominated by a diffractive exchange, with evidence at large $x_{\mathbb{P}}$ for a secondary exchange, consistent with the Regge trajectory containing the f mesons. In a QCD analysis of the F_2^D data, in which parton distributions were ascribed to the pomeron [10] and assumed to evolve according to the DGLAP equations [11], the pomeron structure was found to be dominated by gluons carrying large fractions of the exchanged momentum.

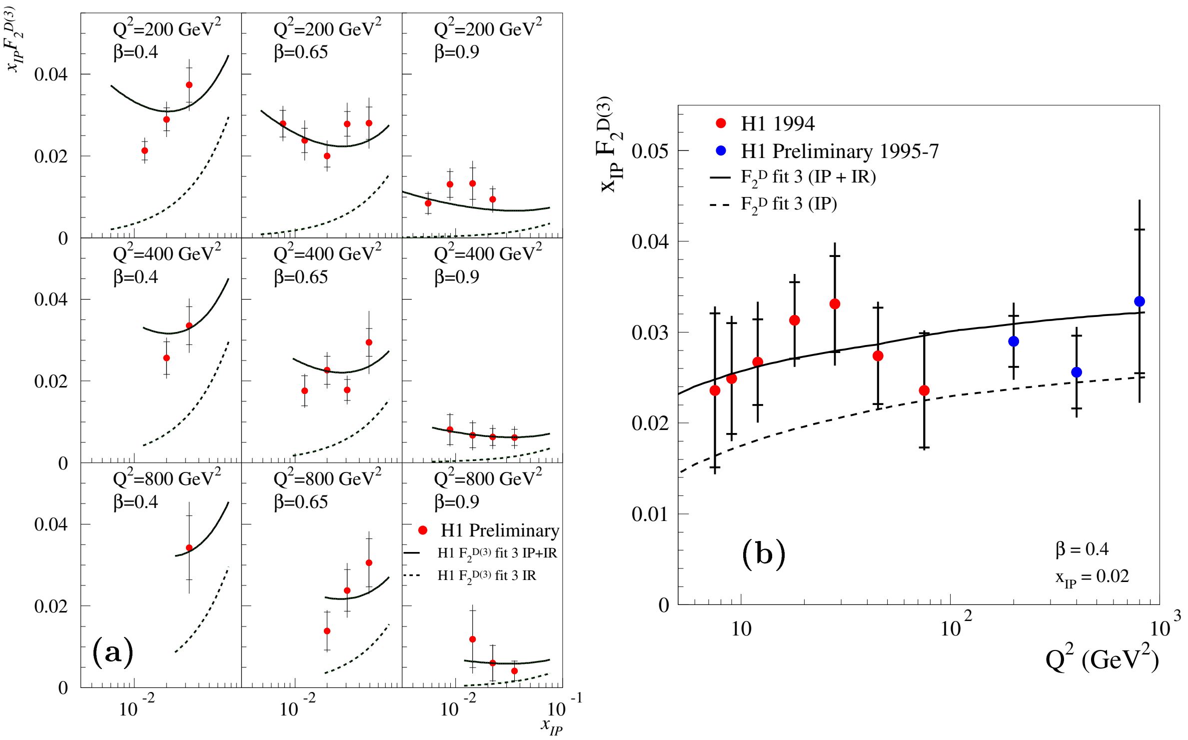

Figure 4: (a) The diffractive structure function shown as a function of $x_{\mathbb{P}}$ in bins of fixed β and Q^2, compared to the extrapolation of a model based on DGLAP fits to lower Q^2 data, in which the pomeron structure is dominated by gluons carrying large fractional momenta. Both pomeron ($\mathbb{P}$) and sub-leading exchange ($\mathbb{R}$) contributions are included. (b) The Q^2 dependence of the diffractive structure function at a fixed value of β and $x_{\mathbb{P}}$, compared to the same model.

A new measurement [12] of $F_2^{D(3)}$ for $Q^2 \leq 800$ GeV^2, using data taken in 1995-7, is shown in figure 4(a). It is compared with predictions based on the pomeron parton distributions extracted from the previous measurement [9], extrapolated to large Q^2 again using the DGLAP equations. The prediction with the sub-leading exchange included is in good agreement with the data. Figure 4(b) shows the Q^2 dependence of $x_{\mathbb{P}} F_2^D$ at a fixed value of $x_{\mathbb{P}}$ and $\beta = 0.4$. The rise in the structure function with Q^2 at such a large value of β lends support to the hypothesis that the pomeron is dominated by gluons carrying large fractional momenta.

3.2 Hadronic Final States of Diffractive DIS

Many final state observables are sensitive to the partonic structure of the diffractive interaction and can be used to test and constrain QCD motivated models. The natural frame in which to study the final state is the rest frame of the system X ($\gamma^\star\mathbb{P}$ centre of mass frame), the natural direction in that frame being the $\gamma^\star\mathbb{P}$ collision axis. First H1 results have appeared on event shapes [13], energy flow and charged particle spectra [14], charged particle multiplicities and their correlations [15], dijet production [16] and charm yields [17]. These measurements have confirmed that the diffractive parton distributions are dominated by gluons carrying large fractions of the exchanged momentum, boson-gluon fusion (BGF) being the dominant hard process. Three examples based on the work of UK physicists are shown below.

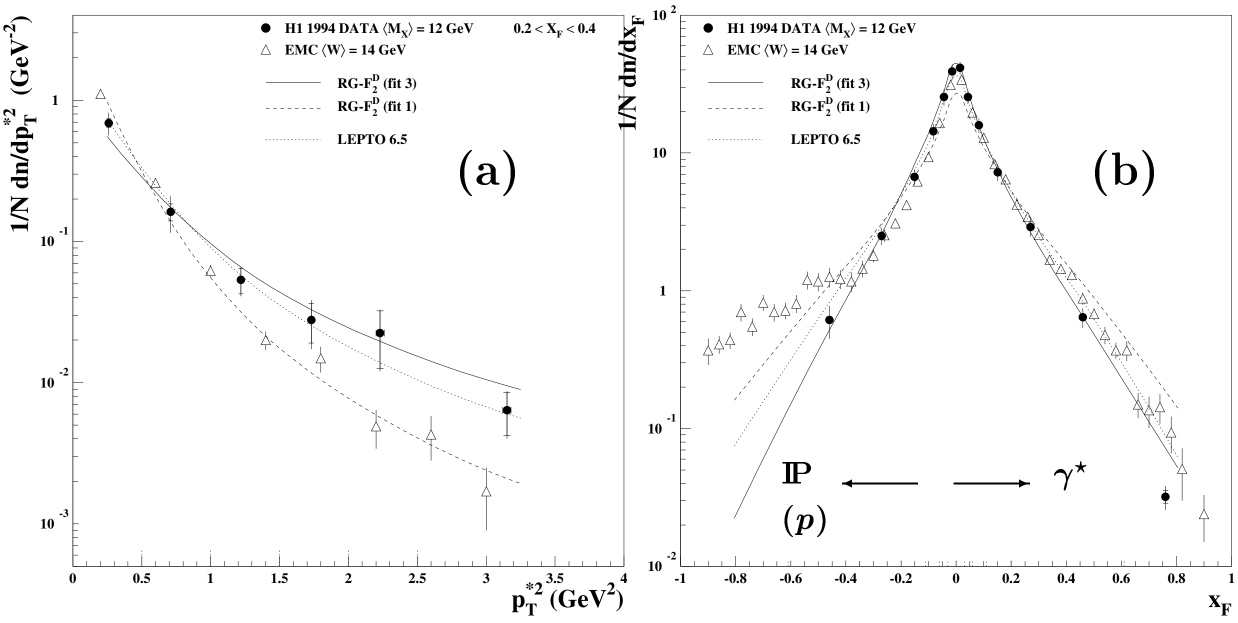

Figure 5: (a) Charged particle transverse momentum distribution for the final state system X in the region $0.2 < x_{\rm F} < 0.4$, compared to μp inclusive DIS data, to the RAPGAP model based on a partonic pomeron with gluon (F_2^D fit 3) and quark (F_2^D fit 1) dominated structure and to a further BGF dominated model, LEPTO. (b) The charged particle $x_{\rm F}$ distribution compared to the same data and models.

Figure 5(a) shows the ${p_T}^2$ distribution of charged particles comprising the system X for the region[1] $0.2 < x_{\rm F} < 0.4$ [14], compared with inclusive μp DIS data at a $\gamma^* p$ centre of mass energy W that is close to M_X in the diffractive data. The μp data correspond to a region in which proton structure is quark dominated. The diffractive data exhibit a significantly harder ${p_T}^2$ distribution than the inclusive DIS data, indicating a larger contribution from processes such as BGF. This is confirmed by comparisons with the RAPGAP Monte Carlo model implementation of the H1 QCD fits to $F_2^{D(3)}$. A good description of the data is obtained only when the pomeron parton distributions are dominated by "hard" gluons.

Figure 5(b) shows the charged particle distribution in $x_{\rm F}$ [14], compared to the same μp data. The $x_{\rm F}$ distribution is approximately symmetric in the diffractive case, with no evidence for the extended remnant in the target direction that is characteristic of lepton-nucleon DIS. Again, the data are well described by the RAPGAP model with gluon dominated pomeron structure.

The study of dijets is particularly sensitive to the gluon induced BGF process. The jet transverse momenta $p_T^{\rm jet}$ introduce a further hard scale to the problem, testing the universality of the parton distributions extracted from F_2^D and allowing hard diffraction to be tested at $Q^2 = 0$ as well as in DIS. Estimators $x_\gamma^{\rm jets}$ and $z_{\rm I\!P}^{\rm jets}$ of the photon and pomeron momenta that are transferred to the dijet system can be obtained as described in [16]. Figure 6(a) shows the $x_\gamma^{\rm jets}$ distribution in photoproduction [16]. There are clear contributions from resolved as well as direct photon interactions. Compared through the POMPYT Monte Carlo model with different sets of pomeron parton distributions, it is clear that quark dominated parton distributions underestimate the dijet rates by large factors. The gluon dominated partons give a fair description of the data with p_T as the factorisation scale. In the region dominated by resolved photon interactions ($x_\gamma^{\rm jets} \lesssim 0.8$), there is some evidence for an excess in the prediction, which may be related to rapidity gap destruction effects [18].

Figure 6(b) shows the $z_{\rm I\!P}^{\rm jets}$ distribution in DIS [16]. There are significant contributions in the region of large $z_{\rm I\!P}^{\rm jets}$, as expected for the dominance of gluons with large fractional momenta

[1]Feynman-x is defined here as $x_{\rm F} = 2p_{\rm L}^\star/M_X$, where $p_{\rm L}$ is the charged particle's longitudinal momentum.

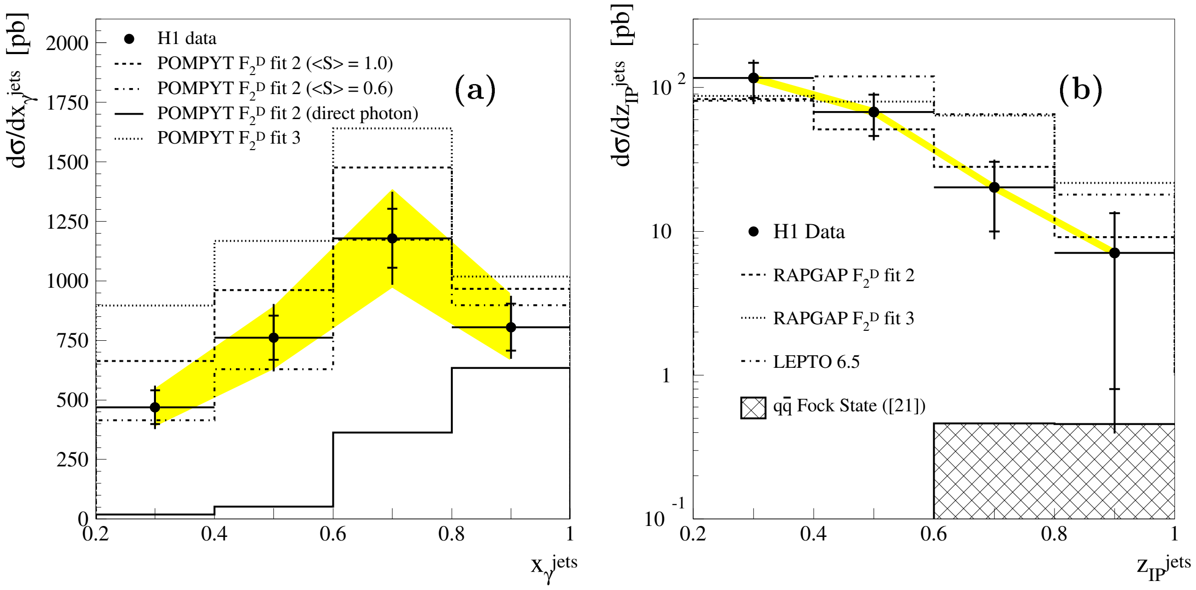

Figure 6: (a) Differential cross section for diffractive dijet photoproduction as a function of $x_\gamma^{\rm jets}$. The data are compared with the predictions of the POMPYT Monte Carlo model, based on two sets of gluon dominated pomeron parton distributions. The effect of possible rapidity gap destruction due to spectator interactions in resolved photon interactions is shown by applying a constant weighting factor $\langle S \rangle = 0.6$ to all resolved photon interactions in the simulation. (b) Differential cross section for diffractive dijet electroproduction as a function of $z_{\rm I\!P}^{\rm jets}$. The data are compared to the RAPGAP model based on two gluon dominated sets of parton distributions, to the LEPTO model in which BGF also dominates and to a prediction based on the exclusive production of $q\bar{q}$ final states.

in the exchange. The large contribution at lower $z_{\rm I\!P}^{\rm jets}$ demonstrates that the final state is more complicated than a simple $q\bar{q}$ pair at lowest order. The data are compared through the Monte Carlo program RAPGAP with the pomeron parton distributions extracted from F_2^D. Once again, the gluon dominated parton distributions give a good description of the data.

The dominance of the BGF process is expected to lead to more copious production of charm in the diffractive final state than would be expected for a quark dominated exchange. Combining data taken in 1995-7, a clear signal is observed for the charmed $D^{*\pm}$ meson in the decay channel $D^{*+} \to D^0 \pi^+_{\rm slow} \to (K^- \pi^+) \pi^+_{\rm slow}$ and its charge conjugate (figure 7) [17]. A cross section of 154 ± 40 (stat.) $\pm$ 35 (syst.) pb is measured for the kinematic range $2 < Q^2 < 100$ GeV^2, $0.05 < y < 0.7$, $x_{\rm I\!P} < 0.04$, $M_Y < 1.6 GeV$ and $|t| < 1$ GeV^2, with $p_T(D^*) > 2$ GeV and $|\eta(D^*)| < 1.5$. This cross section is once again incompatible with predictions based on a quark dominated pomeron.

3.3 Diffraction at Large Momentum Transfer

The region of large $|t|$ is believed to be a particularly good filter for hard diffractive processes in which the pomeron itself may be perturbatively calculable by considering the exchange of a pair of gluons from the proton in a net colour-singlet configuration [19]. A particularly interesting possibility [20] is that the evolution of the two-gluon exchange may be governed by BFKL dynamics [21]. Following measurements of quasi-elastic J/ψ production at large $|t|$ [22] and of rapidity gaps between high p_T jets [23], an analysis has been performed of the inclusive diffractive photoproduction cross section $\gamma p \to XY$ at large t [24]. The kinematic region covered is $165 < W < 233$ GeV, $|t| > 20$ GeV^2 and $y_{\rm I\!P} < 0.018$, where $y_{\rm I\!P} = (M_Y^2 - t)/W^2$. The measured cross section is shown in figure 8. It is found to be much larger than that expected for

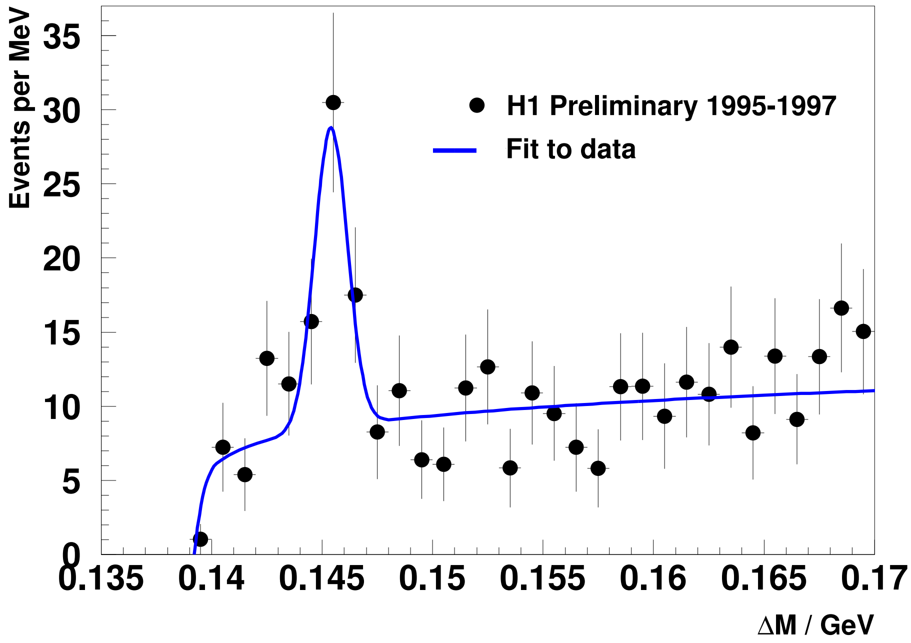

Figure 7: Distribution of the mass difference $\Delta M = M(K^-\pi^+\pi^+_{\mathrm{slow}}) - M(K^-\pi^+)$, showing a clear peak corresponding to the D^* meson. The curve is a fit to a Gaussian with an experimentally motivated background function, yielding 38 ± 10 (stat.) $\pm\, 4$ (syst.) $D*$ mesons in the peak.

the exchange of the soft pomeron as measured in low $|t|$ photoproduction [25]. It is also much larger than that expected from fluctuations in the hadronisation process for non-diffractive photoproduction. Predictions including the exchange of the BFKL pomeron can be made to fit the data.

4 Vector Meson Production

In addition to the above, studies of the exclusive production of both light and heavy vector mesons provide information on the nature of diffraction. A particularly interesting quantity, the distribution in t, has been measured in the photoproduction of J/ψ mesons at HERA for various incident photon energies. Here t is the four momentum transferred from the photon to the J/ψ meson. Such photoproduction could occur via Pomeron exchange, as is the case with vector mesons made from light quarks. However, because of the higher mass of the heavy quarks, it is possible that harder processes may contribute. If the production mechanism is dominated by the first of these then the distribution in t will become steeper as the photon energy increases. On the other hand if hard processes are contributing this may not occur. The steepness of the t distribution is measured by the parameter b shown in figure 9 below. We see that at present the data are not precise enough to establish if the t distribution increases with energy, which is related to the abscissa, W. However, as the precision of these data improve we will be able to give a definite answer to this question.

5 The Hadronic Final State in DIS

The hadronic final state arising from ep interactions is an extremely sensitive environment in which to investigate perturbative and non-perturbative QCD processes. As was already seen for diffractive scattering (section 3.2), hadronic final state studies are complementary to inclusive structure function measurements and provide information on the partonic nature of the incoming hadron. This section presents measurements on jet and particle production in

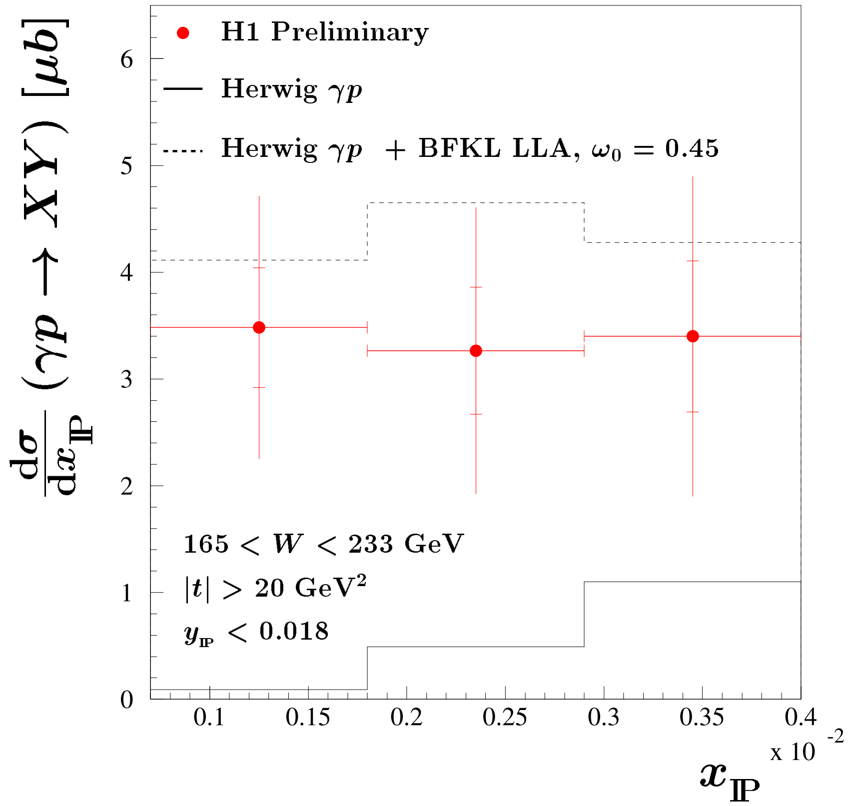

Figure 8: The differential cross section $d\sigma/dx_{\mathbb{P}}$ for the process $\gamma p \to XY$ at large $|t|$, compared to the predictions of a simulation of standard photoproduction processes and to a model containing a hard pomeron calculated using the BFKL equations.

DIS extending beyond the diffractive sector. These studies benefit enormously from the high luminosity produced by HERA in recent years. This has enabled, for the first time, precise high Q^2 measurements of charged particle momentum spectra and allowed the quantitative investigation of QCD scaling violations. Similarly, high transverse momentum particle and jet production can now be studied in more detail and with far greater accuracy than previously possible. With such measurements, the evolution of proton and photon structure over the vast kinematic range provided at HERA can be studied.

5.1 Fragmentation Functions and Rapidity Spectra in the Breit Frame

Studies of DIS *ep* processes in the Breit frame of reference by a hadronic final state analysis group based in the UK have recently been published [26, 27, 28, 29]. These included the energy behaviour of the moments of the fragmentation function, invariant energy spectra and the correlation between the charge of the hadronic final state and the charge of the scattered parton [30]. Two highlights of this years work are described below.

5.1.1 Scaling Violations

In figure 10, the fragmentation function is plotted in intervals of the scaled momentum variable, x_p, as a function of the invariant four-momentum transfer, Q. The function shows a strong rise at small x_p with increasing energy which becomes flatter in the larger x_p region. Predictions based on NLO QCD calculations [31] (dotted line) have a tendency to overestimate the inclusive particle production cross section in the small x_p, low Q region where the available phase space for fragmentation is strongly suppressed. Mass effects are neglected in the pQCD approach but may be taken into account by means of a "power-correction" factor of the form

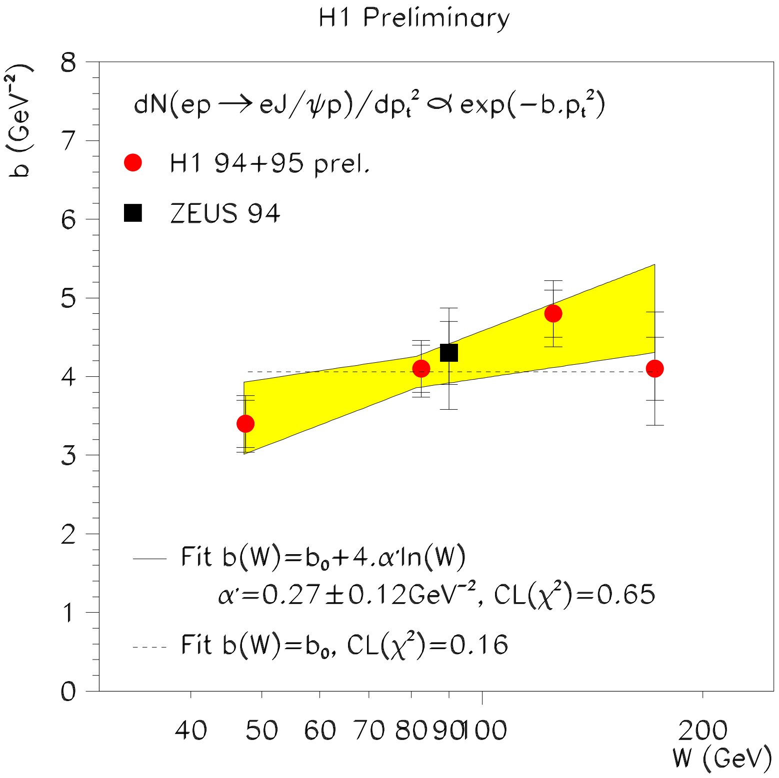

Figure 9: The slope parameter b of the t distribution as a function of the centre of mass energy, W, which is related to the incident photon energy.

$$F = \left(1 + \left(\frac{\mu}{p_h}\right)^2\right)^{-1}$$

suggested by Yuri Dokshitzer at the UK Phenomenology Conference in Durham. Here, p_h is the momentum of the final state hadron and μ is a free parameter that sets the hadronic mass scale.

The solid line in figure 10 shows the result of applying this correction (μ = 300 MeV) to the NLO calculation. The agreement with the H1 ep data over the available phase space is remarkable.

5.1.2 Rapidity Spectra

Figure 11 presents the rapidity spectra [32] for high Q^2 data integrated over all transverse momenta, and binned in various p_t intervals. The proton remnant extends toward large positive rapidity. At low p_t a clear plateau in the target hemisphere can be seen. As the average p_t of the particles increases, QCD effects gradually evolve the flat plateau into an almost Gaussian structure peaking near the origin of the Breit frame axis ($Y = 0$).

Predictions based on Local Parton Hadron Duality indicate the appearance of two distinct plateaux with a 9/4 ratio in their respective heights reflecting the colour charge of the dominant gluonic radiation in the target hemisphere [33] as opposed to the quark in the current region. Despite many tests to isolate events in which such behaviour might be expected to be amplified, we have been unable to observe a double plateau structure.

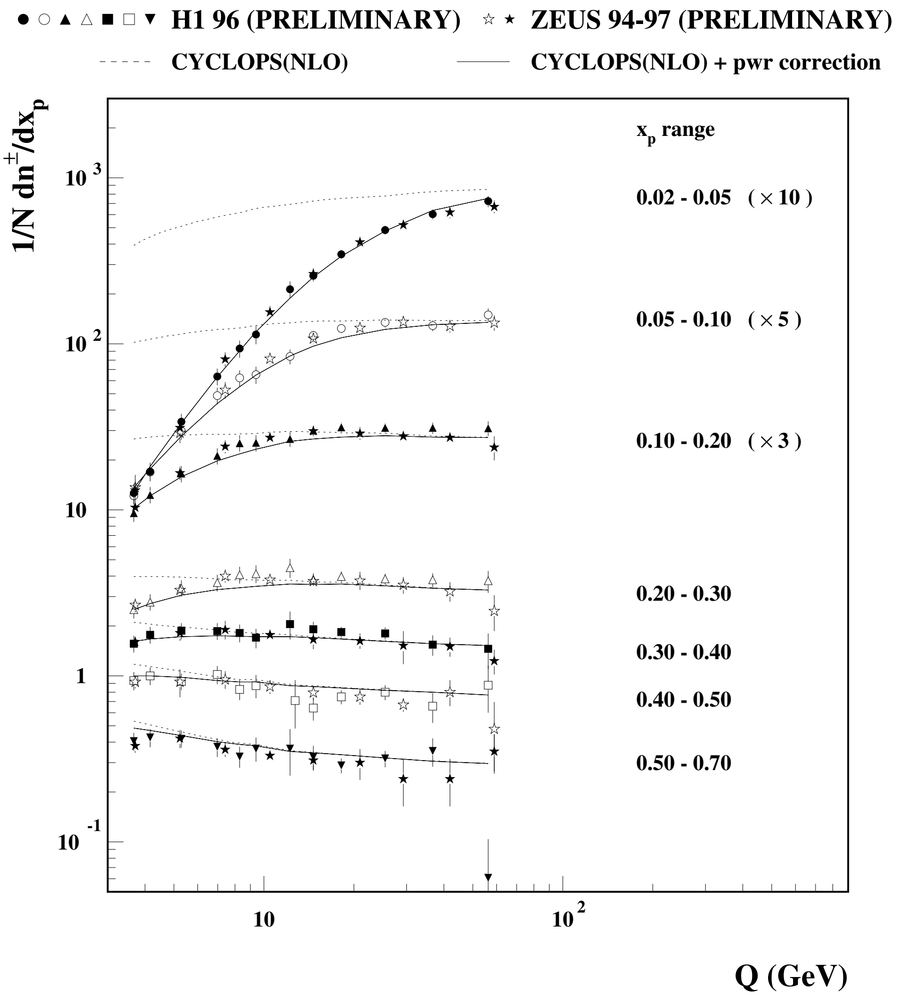

Figure 10: Fragmentation functions plotted for different intervals of x_p as a function of Q and compared with e^+e^- data at equivalent centre-of-mass energies, E^*. Note that the data for the three smallest intervals of x_p are scaled by factors of 10, 5 and 3 for clarity. The dotted and solid lines show the predictions of the CYCLOPS NLO Monte-Carlo calculation with and without the power correction, respectively.

5.2 Forward Particle Production

The hadronic final state in low x DIS processes is a very sensitive environment in which to disentangle different QCD processes. In particular the region near the proton remnant (forward region) will allow new insights to be gained into dynamical features of QCD at low Bjorken-x [34] since it provides a large phase space for parton emissions. Several prescriptions for the QCD dynamics of such emissions have been proposed.

DGLAP [11] evolution in which the relevant evolution parameter is $\log(\frac{Q^2}{Q_0^2})$ and in which emitted partons are strongly ordered in transverse momentum, k_T, has been successfully tested over a wide range of Q^2 and provides a good description of, among other things, the violations of scaling observed in structure function measurements. The BFKL [21] evolution equation,

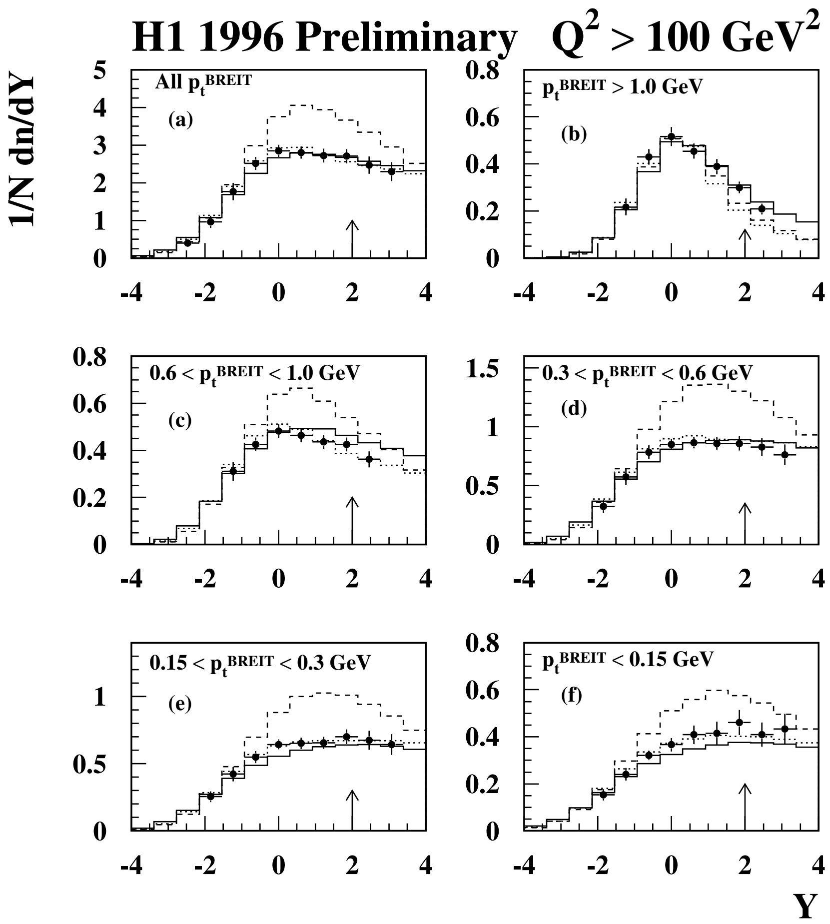

Figure 11: The rapidity distribution for (a) all charged tracks, and (b-f) for the five indicated intervals of track transverse momentum, p_t^{BREIT}, in the Breit frame, all at high Q^2. The arrow indicates the position of the origin of the hadronic centre of mass system for the $< Q >$ (23 GeV) of the data. The histograms show the predictions of LO Monte Carlo models, the solid line utilising a color dipole fragmentation, the dashed (dotted) lines utilising a parton shower with (without) soft colour interaction effects.

where the relevant evolution parameter is $\log(\frac{1}{x})$ and for which there is no ordering in partonic k_T, is expected to become applicable at small enough x when the $\log(\frac{1}{x})$ terms dominate the evolution. CCFM [35] evolution, in which the parton emissions obey angular ordering, is expected to be valid for both low and high Bjorken-x, thereby forming a bridge between the BFKL and DGLAP approaches. Hadronic final state calculations for all three prescriptions are, for the first time, becoming available [36].

It has been noted that another approach, allowing the virtual photon involved in deep inelastic scattering to have hadronic structure, can produce results similar to those obtained in the BFKL approach [37]. The resolved photon picture can be considered to be applicable when the squared transverse momentum of the parton entering the hard scattering process from the proton side is larger than the virtuality, Q^2, of the photon.

A complication in using the hadronic final state to investigate QCD evolution is the effect of soft hadronisation processes and it has been suggested that these can be reduced by studying single high-p_T particle production [38, 39].

Results are presented as spectra in Bjorken-x of single charged particles and π^0-mesons in the range $5^\circ < \theta < 25^\circ$ and $p_T > 1$ GeV, where θ and p_T refer, respectively, to the polar angle and transverse momentum of the particle and are measured with respect to the incoming proton direction. All distributions are normalised to the number of DIS events, N, that fall into the kinematic range: $E_{e'} > 12\,\text{GeV}$, $156° < \Theta_e < 173°$, $y > 0.1$ and $0.0002 < x < 0.00236$. Here $E_{e'}$ and θ_e are the energy and polar angle of the scattered lepton, respectively.

Charged particle results are shown in Fig. 12 (top left) for the lower threshold of $x_{cp} = \frac{E_{cp}}{E_{proton}} > 0.0098$, where E_{cp} and E_{proton} are the charged particle and incoming proton energies respectively.

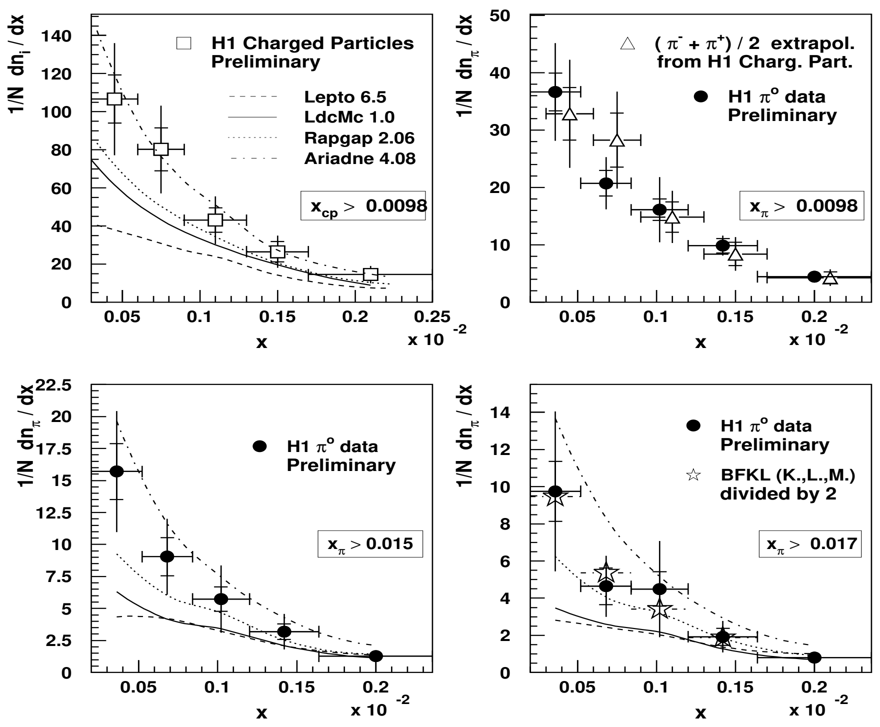

Figure 12: Forward charged particle and π^0 spectra in Bjorken-x for $p_T > 1$ GeV and $5° < \theta < 25°$ are shown for different values of the lower energy threshold $x_{cp} = \frac{E_{cp}}{E_{proton}}$ (charged particles) $x_\pi = \frac{E_\pi}{E_{proton}}$ (π^0-mesons). Here n_{cp} (n_π) is the number of charged particles (π^0-mesons) and N is the number of events that enter the distribution. For comparison, predictions of four different QCD models are overlayed. For the highest x_π bin a BFKL calculation is available. Its predictions have been divided by two for presentation purposes.

The charged particle rate clearly rises with decreasing Bjorken-x providing evidence of much more hard partonic radiation than predicted by DGLAP type QCD models as represented by LEPTO [40]. A reasonable description of the data can be obtained by adding contributions from processes in which the photon is not point-like but acts as a resolved object as is implemented in RAPGAP [41]. The renormalisation and factorisation scales were both set to $p_T^2 + Q^2$ in these calculations where p_T^2 is the transverse momentum squared of the outgoing partons from the hard sub-process. Measurements are also presented, in Fig. 12, for π^0-mesons for the three lower thresholds of $x_\pi >$ [0.0098, 0.015, 0.017]. To check the consistency of the measurements, ARIADNE [42] with JETSET [43] was used to estimate the contribution of charged pions to the charged particle data. The results, divided by two, are compared to the π^0 measurement in Fig. 12 (top right) and are in good agreement. For the first time the data can also be compared to a MC model based on the CCFM approach (LDCMC [36]). Although this is close to the data for the single particle spectra with the lower energy cutoffs, it becomes increasingly similar to the DGLAP based model in the higher energy π^0 spectra.

The Colour Dipole Model, as implemented in ARIADNE, tends to overshoot the data in most of the measured distributions. BFKL calculations, folded with fragmentation functions, are available for the highest momentum π^0 points [44]. These predictions were found to overestimate the observed π^0 yield and the calculated points are shown in Fig. 12 divided by two. Despite this large normalisation discrepancy, the calculations are seen to describe well the x dependence of the π^0 measurements. More details on this analysis can be found in [45].

6 Virtual Photon Structure

Studies of the structure of virtual photons using high transverse momentum (P_t) jets have now been extended to the case where there are two such jets in the final state. The photon, with virtuality Q^2, is probed with a resolution given by the P_t^2 of the jets. With dijet events it is possible to reconstruct x_γ, the fraction of the virtual photon's momentum carried by the parton participating in the hard scattering process. In leading order dijet production, $x_\gamma < 1$ for resolved photon processes and $x_\gamma = 1$ for direct. Because of the presence of two hard scales, Q^2 and P_t^2, and the point-like coupling at the core of the fluctuations leading to the partonic structure of the photon, virtual photon structure is quite unlike that of hadrons. As the probing scale increases, the probability of finding a parton at high x_γ increases. Furthermore, in addition to this unique scaling-violation behaviour, perturbative QCD is also able to predict the evolution of the photon structure with its virtuality in the region $P_t^2 \gg Q^2 \gg \Lambda^2$. Here, the target virtuality provides a natural cut-off, the leading log behaviour of the photon structure is $\sim \ln(P_t^2/Q^2)$ and so the virtual photon parton densities are slowly suppressed as $Q^2 \to P_t^2$. Away from this region, various models have been proposed to interpolate between the low- and high-Q^2 domains [46].

H1 have investigated the virtual photon structure as functions of x_γ, probing scale and target virtuality [47]. The triple-differential cross-section, $\mathrm{d}^3\sigma_{ep}/\mathrm{d}Q^2\mathrm{d}\overline{E_t}^2\mathrm{d}x_\gamma^{jets}$ ($\overline{E_t}^2$ is the mean E_t of the two highest E_t jets and x_γ^{jets} is the value of x_γ calculated from them), was determined and then this was used to measure, for the first time, an effective parton density (EPDF) of the virtual photon. The study spans the range $1.6 < Q^2 < 80\mathrm{GeV}^2$ with $0.1 < y < 0.7$, using data taken in 1996.

Both the triple-differential cross-section and the effective parton density show the characteristic behaviour predicted by models based on perturbative QCD. For example, the cross-section is shown in figure 13 as a function of x_γ^{jets} in ranges of Q^2 and $\overline{E_t}^2$. It decreases rapidly with increasing $\overline{E_t}^2$ and with increasing Q^2 in a manner consistent with the logarithmic suppression inherent in the models of virtual photon structure with which it is compared. The shaded histogram shows the expectation from a model with point-like coupling of photons only. This is clearly unable to describe the data except in the highest x_γ^{jets} bin and possibly also in the highest Q^2 range.

7 Detector Developments

All the components described below remain the responsibility of the UK groups. Each detector requires the continuous attention of dedicated physicists, either resident at DESY or from the UK remotely via computer link. The UK groups have also taken on the task of improving the forward track detector to make it better able to exploit the increased luminosity that HERA

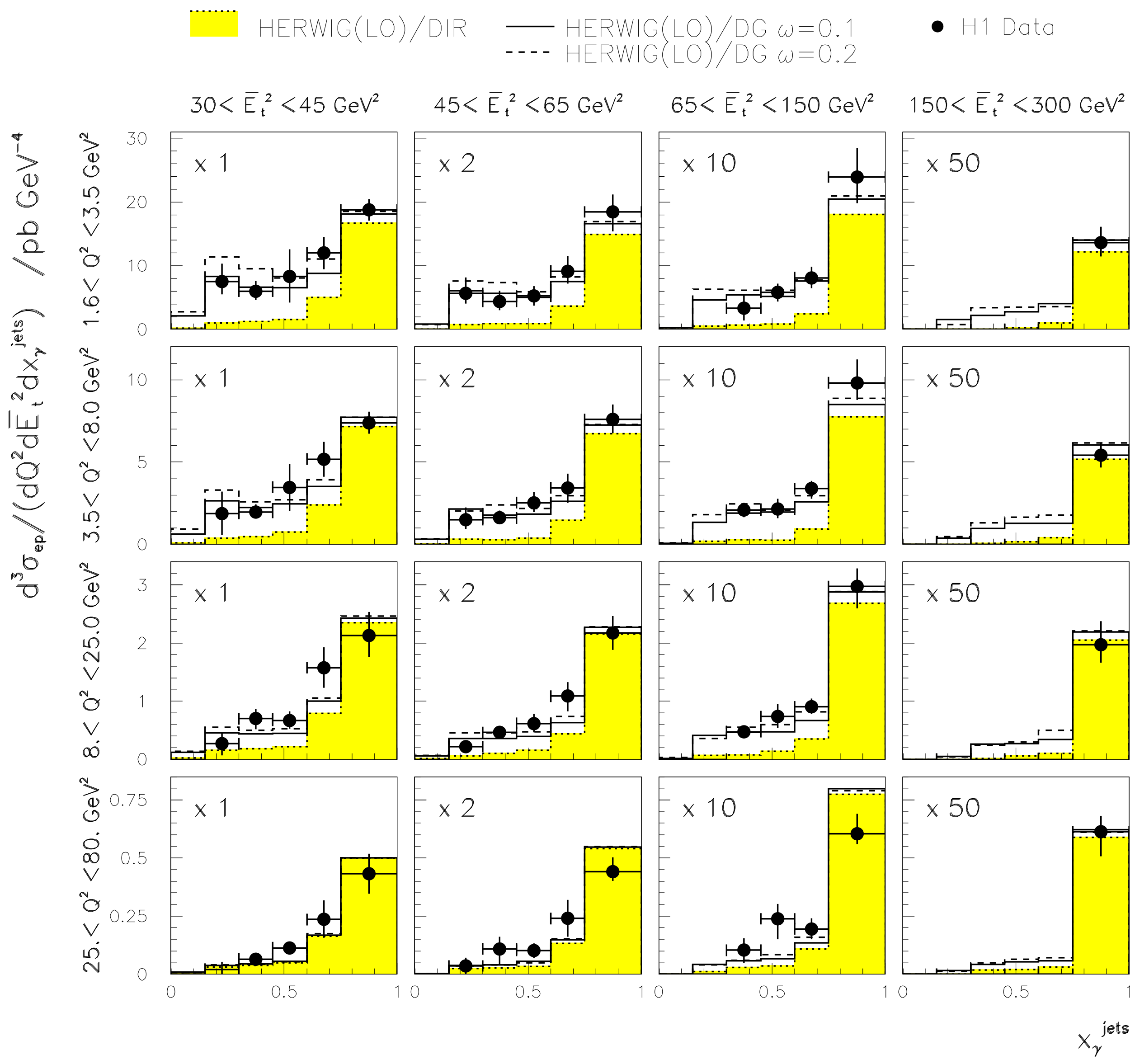

Figure 13: The differential dijet cross-section $d^3\sigma_{ep}/dQ^2 d\overline{E_t}^2 dx_\gamma^{jets}$ shown as a function of x_γ^{jets} for different regions of $\overline{E_t}^2$ and Q^2. Note the indicated scale factors applied to the cross-sections. The error bar shows the quadratic sum of systematic and statistical errors. The absence of a data point indicates that no measurement was made because of insufficient statistics for the two dimensional unfolding. The predictions of various models for virtual photon structure are also shown. The shaded histogram shows the prediction of a model which does not include virtual photon structure.

will deliver from the start of the year 2001.

7.1 Data Acquisition and Silicon Tracker Readout

During 1998, the data acquisition and readout systems, for which RAL are responsible, continued to operate and perform reliably. These systems, which are based on the VMEbus standard, have been described extensively in previous annual reports. Optical fibres are used to interconnect over 100 electronics crates containing the necessary analogue to digital converters and several hundred microprocessing elements. Over the last two years, the introduction of the PCI standard has considerably enhanced the system potential which, together with the latest Power PC technology, has resulted in ever more compact solutions performing at increased data throughput rates.

7.2 Backward Calorimeter Timing

Since installation and commissioning in 1995, the timing electronics has functioned reliably and well. Despite the increase in the proton current and inevitable associated background, the good timing has enabled even low energy electron events to be reliably triggered with low background rates.

7.3 Forward Muon Detector and Trigger

Both the forward muon detector and the forward muon detector trigger have continued to function reliably and efficiently throughout the year.

7.4 Forward Track Detector

Throughout 1998 the forward track detector (FTD) has functioned reliably. A new readout system, which enabled the hit finding algorithm to be performed online, was fully commissioned this year. As a consequence the H1 data taking purity has been improved and the online processing time reduced.

In order to enhance the performance of the FTD following the HERA upgrade, it is planned to remove the transition radiators and the multi-wire proportional chambers and replace these with additional planar chambers. Although it has been demonstrated that the transition radiators and the radial chambers are able to provide improved electron identification in the forward direction, this facility has proved to be of no practical significance in physics analyses, as the amount of material before the FTD means that the majority of primary electrons induce electromagnetic showers before entering the FTD. The multi-wire proportional chambers, used in the H1 z-vertex and forward ray triggers, will be largely redundant following the installation of the new central inner proportional chamber system in the year 2000. The additional planar chambers will allow resolution of the majority of the ambiguities limiting the efficiency of track finding in the current FTD and make H1 better able to study many topics of interest following the HERA luminosity upgrade, for example the production of charm, identified via the $D^{*+} \rightarrow D^0\pi^+_{\rm slow} \rightarrow K^-\pi^+\pi^+_{\rm slow}$ decay chain, in the forward direction. To allow improved triggering in the forward region, scintillator arrays before and after the FTD are also to be constructed. These will further improve the performance of the FTD by allowing more precise calibration with cosmic ray events for which the crossing time, t_0, is accurately known.

The detailed design of the new planar chambers was completed in 1998. Orders for many of the major components have been, or are about to be, placed. The chambers are to be built at the Daresbury Laboratory and construction and testing facilities are being prepared there. In parallel with the above, preparation of the necessary monitoring, read-out, simulation and reconstruction software is proceeding. The scintillator and wave-length shifter for the new trigger has been purchased and tests of various possible readout schemes are being done. It is currently expected that the necessary chambers and other hardware for the FTD, the new trigger and the attendant software will be ready for installation by the beginning of the year 2000.

8 Summary

The UK groups within H1 have played a leading role in both the physics studies undertaken by the collaboration in 1998 and the operation of the detector. The contributions of the UK to the upgrade of the H1 detector are designed to ensure that this role can be maintained following the HERA luminosity upgrade, ensuring our involvement in an exciting physics programme until well into the next millenium.

References

[1] H1 Collab., C. Adloff et al., Z. Phys **C74** (1997) 191.

[2] A. Arbuzov et. al., DESY 95-185, hep-ph/9511434.

[3] CTEQ Collab. MSUHEP-60426, CTEQ-604.

[4] A. Martin et. al., RAL-TR-98-029, hep-ph/9803445.

[5] W. Hollik et. al., Proceedings of the Workshop Physics at HERA, vol. 1, eds. W.Buchmüller, G.Ingelman, DESY (1992) 923-946.

[6] R.M Barnett et al., Phys. Rev. D1 (1996) 54.

[7] H1 Collab., S. Aid et al., Nucl. Phys. **B470** (1996) 3.

[8] K. Goulianos, Phys. Rep. **101** (1983) 169.

[9] H1 Collaboration, C. Adloff et al., Z. Phys. **C76** (1997) 613.

[10] G. Ingelman, P. Schlein, Phys. Lett. **B152** (1985) 256.

[11] V. Gribov, L. Lipatov, Sov. J. Nucl. Phys. **15** (1972) 438 & 675.
Yu. Dokshitzer, JETP **46** (1977) 641.
G. Altarelli, G. Parisi, Nucl. Phys. **B126** (1977) 298.

[12] H1 Collaboration, Conf. Paper 571, 29th Intern. Conf. on HEP, Vancouver, Canada (1998).

[13] H1 Collaboration, C. Adloff et al., Eur. Phys. J. **C1** (1998) 495.

[14] H1 Collaboration, C. Adloff et al., Phys. Lett. **B428** (1998) 206.
C. Cormack, Ph.D. thesis, University of Liverpool 1997 (unpublished).

[15] H1 Collaboration, C. Adloff et al., Eur. Phys. J. **C5** (1998) 439.

[16] H1 Collaboration, C. Adloff et al., DESY **98-092**, Submitted to Eur. Phys. J.

[17] H1 Collaboration, Conf. Paper 558, 29th Intern. Conf. on HEP, Vancouver, Canada (1998). P. Thompson, Ph.D. thesis, University of Birmingham, in litt.

[18] J. Bjorken, Phys. Rev. **D47** (1993) 101.
E. Gotsman, E. Levin, U. Maor, Phys. Lett. **B309** (1993) 199.
E. Gotsman, E. Levin, U. Maor, TAUP 2485-98, hep-ph/9804404.

[19] F. Low, Phys. Rev. **D12** (1975) 163.
S. Nussinov, Phys. Rev. Lett. **34** (1975) 1286.

[20] A. Mueller, W. Tang, Phys. Lett. **B284** (1992) 123.
B. Cox, J. Forshaw, Phys. Lett. **B434** (1998) 133.

[21] E. Kuraev et al., Sov. Phys. JETP **45** (1977) 199.
Y. Balitsky, L. Lipatov, Sov. J. Nucl. Phys. **28** (1978) 822.
L. Lipatov, Sov. Phys. JETP **63** (1986) 904.

[22] H1 Collaboration, paper 274 at Int. Europhys. Conf. on HEP, Jerusalem, August 1997.

[23] H1 Collaboration, paper 380 at Int. Europhys. Conf. on HEP, Jerusalem, August 1997.

[24] H1 Collaboration, Conf. Paper 570, 29th Intern. Conf. on HEP, Vancouver, Canada (1998). B. Cox, Ph. D. thesis, University of Manchester, 1998 (unpublished).

[25] H1 Collab., C. Adloff et al., Zeit. Phys. **C74** (1997) 221.

[26] H1 Collaboration, C. Adloff et al., 29th International Conference on High Energy Physics ICHEP98, Vancouver, Canada, July 1998 No. 531

[27] P. Dixon, D. Kant and G. Thompson, Fragmentation Function Scaling Violations in the Breit Frame, submitted for the proceedings of the 3rd UK Phenomenology Workshop 20th-25th September 1998

[28] K.T. Donovan, D. Kant and G. Thompson, Rapidity Plateaux in the Breit Frame, submitted for the proceedings of the 3rd UK Phenomenology Workshop 20th-25th September 1998

[29] D. Kant, QCD Studies in the Breit Frame at HERA, Nucl. Phys. B (Proc. Suppl.) 71 (1999) 31-38.

[30] R.K. Griffiths, Ph.D thesis, University of London, 1998

[31] D. Graudenz, CERN TH/96-52, CERN TH/96-155 (hep-ph/9606460), CERN TH/96-187 (hep-ph/9610287)

[32] K.T. Donovan, Ph.D thesis, University of London, 1998.

[33] W. Ochs, Proceedings of the Ringberg Worshop "New Trends in HERA Physics", Tegernsee, Germany, 25-30 May 1997 hep/ph/9709248.

[34] A.H. Mueller, Nucl. Phys. B (Proc. Suppl.) 18C (1990) 125;
A.H. Mueller, J. Phys. G17 (1991) 1443;
J. Kwieciński, A.D. Martin, P.J. Sutton, Phys. Lett. B325 (1994) 212.

[35] M. Ciafaloni, Nucl. Phys. B296 (1987) 259;
S. Catani, F. Fiorani, G. Marchesini, Phys. Let. 234B (1990) 339;
S. Catani, F. Fiorani, G. Marchesini, Nucl. Phys. B336 (1990) 18.

[36] W.J. Stirling, hep-ph/9804431.
G. Salam, hep-ph/9805322.
L. Lönnblad, JHEP 03 (1998) 006; hep-ph/9709424.

[37] H. Jung, L. Jönsson, H. Küster, DESY 98-051.

[38] M. Kuhlen, Phys. Lett. B382 (1996) 441.

[39] J. Kwiecinski, S.C. Lang and A.D. Martin, hep-ph/9707240.

[40] G. Ingelman, A. Edin, J. Rathsman, Comp. Phys. Comm. 101 (1997) 108.

[41] H. Jung, Comp. Phys. Comm. 86 (1995) 147
http://www-h1.desy.de/~jung/rapgap.html

[42] L. Lönnblad, Comp. Phys. Comm. 71 (1992) 15.

[43] T. Sjöstrand, Comp. Phys. Comm. 39 (1986) 347;
T. Sjöstrand and M. Bengtsson, Comp. Phys. Comm. 43 (1987) 367.

[44] J. Kwiecinski, S.C. Lang, A.D. Martin, Phys. Rev. D55 (1997) 1273.

[45] 1 Collab., C. Adloff et al., DESY-98-143, Accepted by Nuc. Phys. B.

[46] T. Sjöstrand and G. A. Schuler, Phys. Lett. **B376** (1996) 193;
M. Glück, E. Reya and M. Stratmann, Phys. Rev. **D54** (1996) 5515;
M. Drees and R. Godbole, Phys. Rev. **D50** (1994) 3124;
F. Borzumati and G. Schuler, Z. Phys. **C58** (1993) 139.

[47] H1 Collaboration, "Measurement of Di-Jet Cross-Sections at Low Q^2 and the Extraction of an Effective Parton Density for the Virtual Photon", DESY preprint 98-205 submitted to Eur. Phys. J. C.

H1 Publications 1997

The following have been published by the H1 Collaboration in the period November 1997 to December 1998.

1. "Photo-production of $\Psi(2S)$ Mesons at HERA", Phys.Lett. B415 (1997) 418-434

2. "Hadron Production in Diffractive Deep Inelastic Scattering", Phys. Lett. B428 (1998) 206-220

3. "Multiplicity Structure of Hadronic Final States in Diffractive Deep-Inelastic Scattering at HERA", Eur. Phys. J. C 5 (1998) 3, 439-452

4. "Observation of Events with an Isolated High Energy Lepton and Missing Transverse Momentum at HERA", Eur. Phys. J. C 5 (1998) 4, 575-584

5. "Differential (2+1) Jet Rates and Determination of α_s in Deep-Inelastic Scattering at HERA", Eur. Phys. J. C 5 (1998) 4, 625-639
6. "Di-Jet Event Rates in Deep-Inelastic Scattering at HERA", DESY-98-076 / submitted to Eur. Phys. J. C
7. "Multi-Jet Event Rates in Deep-Inelastic Scattering and Determination of the Strong Coupling Constant", DESY-98-087 / submitted to Eur. Phys. J. C
8. "Diffractive Dijet Production at HERA", DESY-98-092 / submitted to Eur. Phys. J. C
9. "Forward Jet and Particle Production at HERA", DESY-98-143 / submitted to Nucl. Phys. B
10. "Charged Particle Cross Sections in Photoproduction and Extraction of the Gluon Density in the Photon", DESY-98-148 / submitted to Eur. Phys. J. C
11. "Measurement of Leading Proton and Neutron Production in Deep Inelastic Scattering at HERA", DESY-98-169 / submitted to Eur. Phys. J. C

Theses Submitted in 1998

The following theses were submitted by students from the UK Institutes within the H1 collaboration during the period November 1997 to December 1998.

1. "Elastic J/ψ Photoproduction and the Detection and Trigerring of Muons al Low W using the H1 Detector", Kirstee Hewitt (Birmingham).
2. "Charged Particle Transverse Momentum Spectra in Positron Proton Collisions at the H1 Experiment", Theo Holtom (Liverpool).
3. "Rho prime Electroproduction at HERA", Stuart Cocks (Liverpool).
4. "Measurement of the Cross Section for the Elastic Photoproduction of the J/ψ Meson at HERA", M. Anderson (Manchester).
5. "Double Diffraction Dissociation at Large Momentum Transfer", B. Cox (Manchester).
6. "The First Measure of Relative Partonic Contributions in DIS at HERA using an Average Hadronic Charge", Robert K. Griffiths (QMW).
7. "Hadronic Fragmentation Studies in ep Scattering at HERA", Keith T. Donovan (QMW).

H1 Conference Presentations 1998

Conference presentations (from November 1997) by members of the H1–UK groups which are concerned with all aspects of H1 physics and operation are listed below.

1. B. Cox, "Jets and Rapidity Gaps at HERA", in Proc. 3^{rd} LAFEX International School on High Energy Physics, Rio, February 1998.
2. B. Cox, "VDM Production at HERA", in Proc. 3^{rd} LAFEX International School on High Energy Physics, Rio, February 1998.

3. S. Maxfield, “Jets and the Hadronic Final State at HERA”, in Proc. 12^{th} Rencontre de Physique de la Vallee D’Aoste, Aosta Valley, Italy, March 1998.

4. P. Newman,“Inclusive Diffraction and Leading Baryon Production at HERA”, in Proc. 34^{th} Rencontres de Moriond, Les Arcs, France, March 1998.

5. T. Greenshaw, “Recent Results from H1”, in Proc. 6^{th} International Workshop on Deep Inelastic Scattering and QCD, Brussels, April 1998.

6. B. Waugh, “Diffractive Final States”, in Proc. 6th International Workshop on Deep Inelastic Scattering and QCD, Brussels, April 1998.

7. P. Thompson, “Heavy Vector Mesons at HERA”, in Proc. 6th International Workshop on Deep Inelastic Scattering and QCD, Brussels, April 1998.

8. B. Cox, “Rapidity Gaps between Jets at HERA”, in Proc. 6th International Workshop on Deep Inelastic Scattering and QCD, Brussels, April 1998.

9. A. Mehta, “Structure Functions at HERA”, in Proc. 6th International Workshop on Deep Inelastic Scattering and QCD, Brussels, April 1998.

10. E. Rizvi, “QCD Analysis of Structure Funcions”, in Proc. 6th International Workshop on Deep Inelastic Scattering and QCD, Brussels, April 1998.

11. B. Cox, “Isolating the Hard Pomeron at HERA”, talk given at the Institute of Physics Conference, Manchester, April 1998.

12. K. Donovan, “Charged Particle Spectra in the Breit Frame at HERA”, talk given at the Institute of Physics Conference, Manchester, April 1998.

13. M. Smith, “Low Q^2 Jet Production at HERA”, talk given at the Institute of Physics Conference, Manchester, April 1998.

14. P. Thompson, “D^* Production in Diffractive DIS with the H1 Detector”, talk given at the Institute of Physics Conference, Manchester, April 1998.

15. J. Dainton, “The Future of ep Physics at HERA”, talk given at “Aspects of Deep Inelastic Scattering”, Berlin-Zeuthen, June 1998.

16. T. Greenshaw, “QCD at HERA”, invited contribution presented at the High Energy Physics Forum, Abingdon, June 1998.

17. D. Milstead, “Forward Jet and Particle Production at HERA”, talk given at “Aspects of Deep Inelastic Scattering”, Berlin-Zeuthen, June 1998.

18. D. Kant, “Fragmentation Functions and Event Shapes in the Breit Frame”, talk given at “Aspects of Deep Inelastic Scattering”, Berlin-Zeuthen, June 1998.

19. J. Phillips, “H1 Physics Results”, talk given to Extended Scientific Council, DESY, Hamburg, June, 1998.

20. C. Hilton, “Heavy Vector Meson Production at HERA”, in Proc. 3^{rd} International Conference on Hyperons, Charm and Beauty, Geneva, July, 1998.

21. D. Milstead, “Forward Jet and Particle Production at HERA”, in Proc. 29^{th} International Conference on High Energy Physics, Vancouver, July 1998.

22. D. Milstead, “QCD in the Hadronic Final State at HERA”, in Proc. 28^{th} International Symposium on Multi-particle Dynamics, Delphi, Greece, September 1998.

23. P. Newman, “Diffractive Phenomena in ep Physics”, in Proc. International Conference on Hadron Structure, Stara Lesna, Slovakia, September 1998.

24. B. Cox, “Rapidity Gaps between Jets”, in Proc. 4th Workshop on Small-x and Diffractive Physics, Fermilab, US, September 1998.

25. B. Cox, “Experimental Results in Small x Physics and Diffraction”, talk given at the Workshop on HERA Physics, Durham, September 1998, to appear in J. Phys. G.

26. D. Kant, “Can we see the Signature of LPHD Resolvable Gluons at HERA?”, talk given at the Workshop on HERA Physics, Durham, September 1998, to appear in J. Phys. G.

27. P. Dixon, “Scaling Violation of *ep* DIS Fragmentation Functions at HERA”, talk given at the Workshop on HERA Physics, Durham, September 1998, to appear in J. Phys. G.

28. G. Thompson, “Jets and Fragmentation”, summary talk given at the Workshop on HERA Physics, Durham, September 1998, to appear in J. Phys. G.

H1 Conference Submissions 1998

The following papers were submitted by the H1 collaboration to the 29^{th} International Conference on High Energy Physics, Vancouver, July, 1998.

1. Abstract 520: “Measurement of Dijet Cross Sections in Deep Inelastic Scattering at HERA”

2. Abstract 523: “Di-jet Rates in Deep Inelastic Scattering at HERA”

3. Abstract 527: “Multi-Jet Event Rates in Deep-Inelastic Scattering and Determination of the Strong Coupling Constant”

4. Abstract 528: “Differential (2+1) Jet Rates and Determination of α_s in Deep-Inelastic Scattering at HERA”

5. Abstract 529: “Forward Jet and Particle Production at HERA”

6. Abstract 530: “Measurement of Event Shape Variables in Deep Inelastic *ep* Scattering at HERA”

7. Abstract 531: “Evolution of ep Fragmentation and Multiplicity Distributions in the Breit Frame”

8. Abstract 532: “Measurement of Internal Jet Structure in Dijet Production in Deep Inelastic Scattering and Photoproduction”

9. Abstract 533: “Measurement of Inclusive Cross Sections for Neutral and Charged Current Interactions at High-Q^2”

10. Abstract 534: "Precision Measurement of the Inclusive Deep Inelastic ep Scattering Cross Section at Low Q^2 at HERA"
11. Abstract 535: "Low Q^2 – Intermediate x Structure Function Measurement at HERA"
12. Abstract 544: "Measurement of Di-jet Cross-sections in Low Q^2 Deep-Inelastic Scattering Processes at HERA and the Extraction of an Effective Parton Density of the Virtual Photon"
13. Abstract 549: "Dijet Cross Sections in Photoproduction and Determination of the Gluon Density in the Photon"
14. Abstract 551: "High P_t Charged Particle Cross Section in Photoproduction and Extraction of the Gluon Density in the Photon"
15. Abstract 553: "Transverse Energy Production in Deep-Inelastic Scattering"
16. Abstract 556: "Measurement of the Baryon-Antibaryon Asymmetry in Photoproduction at HERA"
17. Abstract 576: "Inclusive Photoproduction of π^0 Mesons in the Photon Hemisphere at HERA"
18. Abstract 578: "Observation of Events with an Isolated High Energy Lepton and Missing Transverse Momentum at HERA"
19. Abstract 579: " Search for Leptoquark Bosons in DIS at High Q^2 at HERA"
20. Abstract 580: "A Search for Squarks of R-Parity Violating SUSY at HERA"
21. Abstract 581: "Search for Excited Fermions at HERA"
22. Abstract 584: "A Search for Contact Interactions in Neutral Current Scattering at HERA"
23. Abstract 585: "Antideuteron Production at HERA and Search for Heavy Stable Charged Particles"